ELSEVIER

Polymer 43 (2002) 4365–4373

polymer

www.elsevier.com/locate/polymer

Morphology, thermal relaxations and mechanical properties of layered silicate nanocomposites based upon high-functionality epoxy resins

Ole Becker[a], Russell Varley[b], George Simon[a,*]

[a]*School of Physics and Materials Engineering, Monash University, Clayton, Vic. 3800, Australia*
[b]*CSIRO Molecular Science, Clayton, Vic. 3169, Australia*

Received 11 December 2001; received in revised form 30 January 2002; accepted 17 April 2002

Abstract

This paper investigates the possibility of improving the mechanical properties of high-functionality epoxy resins through dispersion of octadecyl ammonium ion-modified layered silicates within the polymer matrix. The different resins used are bifunctional diglycidyl ether of bisphenol-A (DGEBA), trifunctional triglycidyl *p*-amino phenol (TGAP) and tetrafunctional tetraglycidyldiamino diphenylmethane (TGDDM). All resins are cured with diethyltoluene diamine (DETDA). The morphology of the final, cured material was probed by wide-angle X-ray scattering, as well as optical and atomic force microscopy. The α- and β-relaxation temperatures of the cured systems were determined using dynamic mechanical thermal analysis. It was found that the presence of organoclay steadily decreased both transition temperatures with increasing filler concentration. Further, the effect of different concentrations of the alkyl ammonium-modified layered silicate on the toughness and stiffness of the different epoxy resins was analyzed. All resin systems have shown improvement in both toughness and stiffness of the materials through the incorporation of layered silicates, despite the fact that it is often found that these two properties cannot be simultaneously achieved. © 2002 Elsevier Science Ltd. All rights reserved.

Keywords: Nanocomposites; Layered silicates; Epoxy resins

1. Introduction

Although mica-type, layered silicates have been used as polymer fillers and process additives for a long time [1,2], it is only since the pioneering work of Toyota researchers [3,4] that these materials are more widely being used to improve the mechanical properties of polymer composites.

The fundamental principle behind nanocomposite formation is that the polymer or its monomers, respectively, are able to move in and (in case of insitu polimerization) react within the interlayer galleries of the layered silicate. Only if the nature and polarity of the inter-gallery ions, matches with the polymer or its monomers, respectively, and the increase in entropy of the organo-ions on gallery separation is sufficient, will the molecules *intercalate* into the gallery. If the layers are completely delaminated by the incoming material, a true nanocomposite will result with the silicate layers fully dispersed throughout the matrix. This process is commonly termed *exfoliation*. To enable swelling or intercalation and exfoliation, respectively, of the layered silicate, the inorganic interlayer cations have to be exchanged by hydrophobic organic cations, which are usually of the alkyl ammonium group. Kornmann et al. [5] recently described the exfoliation mechanism of the silicate platelets in epoxy resins as follows: the driving force for the initial resin intercalation or diffusion into the clay galleries is the high surface energy of the clay, which attracts the polar resin molecule. Without any interlayer reaction thermodynamic considerations would determine the amount of diffusion between the clay platelets to certain amount. Once the interlayer reaction occurs, the polarity of the resin is reduced and further molecules diffuse into the galleries pushing the silicate layers apart and finally exfoliate the clay platelets. At the same time, cure outside the clay galleries occurs, inhibiting migration of more epoxy resin and amines into the galleries until further distribution of the silicate is fixed at the gel point [6]. Therefore the appropriate balance between inter- and extra-gallery reactions, together with the resin and amine diffusion, are the key factors to control the organoclay exfoliation.

Pinnavaia et al. [7,8] have stated that flexible epoxy resin systems with low glass transition temperatures

---

* Corresponding author. Fax: +61-3-9905-4940.
E-mail address: george.simon@spme.monash.edu.au (G. Simon).

PII: S0032-3861(02)00269-0

Table 1
Epoxy resins and hardener as used for the nanocomposite synthesis

Substance	Formula
DGEBA	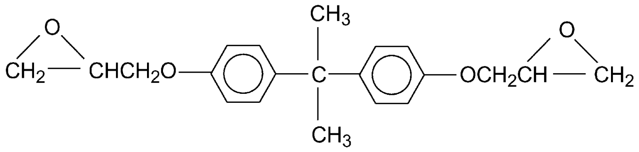
TGAP	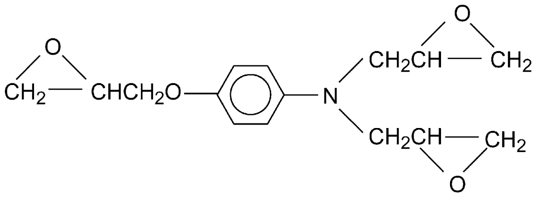
TGDDM	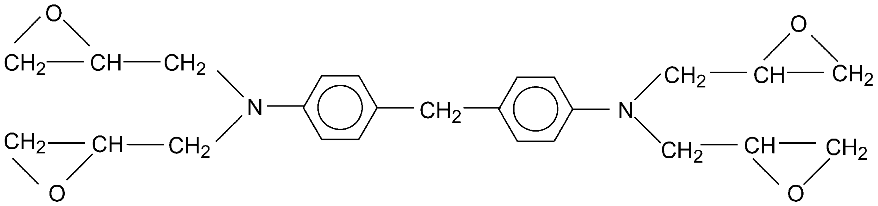
DETDA	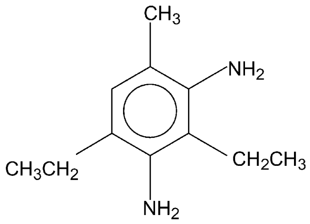 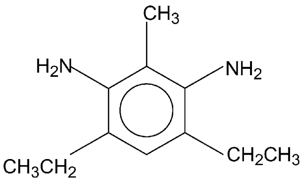

show a much higher increase in modulus and tensile strength by organoclay incorporation, in comparison with those epoxy systems that exhibit a high glass transition. Most of the focus to date on epoxy systems has been on bifunctional resins, predominantly using the well-known diglycidyl ether of bisphenol-A (DGEBA) [5,8–20]. However, more highly crosslinked systems are difficult to toughen and a smaller increase than those achieved for flexible and low glass transition epoxy systems may still prove to be beneficial, in comparison to using higher concentrations of more commonly used fillers.

Although DGEBA is widely used, most aerospace materials and other high-performance applications demand epoxies of higher functionality due to the required higher modulus and glass transition temperature. Along with the DGEBA resin, this paper will investigate the effect of organoclay on two resins of higher functionality, the trifunctional triglycidyl *p*-amino phenol (TGAP) and the tetrafunctional tetraglycidyldiamino diphenylmethane (TGDDM). The curing agent used is the aromatic diethyltoluene diamine (DETDA) which is also widely used in high-performance epoxy resin systems.

2. Experimental

2.1. Materials

The clay used in this study is a commercially available octadecyl ammonium ion-modified montmorillonite layered silicate of Nanocor Inc. (Nanomer I.30E), with an initial interlayer *d*-space of 23 Å. Three different epoxy resins were used as the polymer matrix: DGEBA, DER 331 Dow epoxy resin, TGAP, Araldite MY 0510 of Ciba Speciality Chemicals and the tetrafunctional TGDDM Araldite MY 720 of Ciba Speciality Chemicals. The hardener Ethacure 100, of Albemarle Corp. is a mixture of two DETDA isomers, containing 74–80% 2,4 isomer and 18–24% 2,6 isomer. The structures of the different resins and the amine are illustrated in Table 1.

2.2. Preparation of epoxy–nanocomposites

Chemicals were dried for 24 h at 50 °C under vacuum prior to sample preparation. The layered silicate was dispersed in the resin at 80 °C using a stirrer at 500 revolutions per minute (rpm). After mixing the resin/clay blend for 30 min the curing agent was added and mixed under vacuum for another 60–90 min at approximately 70 °C. The blends were cured for 2 h at 100 °C, 1 h at 130 °C, 12 h at 160 °C followed by a postcure for 2 h at 200 °C. An epoxide to amine ratio of 1:0.9 was chosen for each nanocomposite to ensure an excess of epoxide groups. This is a common industrial practice as non-reacted amine groups present after cure can have some deleterious effects upon the final material [21].

2.3. Nanocomposite characterization

Wide-angle X-ray diffraction (XRD) analyses were performed on a Rigaku Geigerflex generator with a wide-angle goniometer. An acceleration voltage of 40 kV and a current of 22.5 mA were applied using Ni filtered Cu Kα radiation.

The loss tangent, tan δ, of the nanocomposites was determined on a Rheometric Scientific dynamic mechanical thermal analyzer, DMTA IV. The cured samples were clamped in a medium frame using a small center clamp in the dual cantilever mode. Frequency sweep scans were performed from -100 to 50 °C and from 50 to 300 °C at 2 °C/min using frequencies of 1, 3 and 10 Hz.

Differential scanning calorimetry (DSC) temperature scans were taken after cure using a Perkin Elmer DSC-7. The DSC was calibrated with indium and zinc standards. Samples of about 5 mg were sealed in aluminum pans and heated from 50 to 300 °C at a scanning rate of 10 °C/min under nitrogen atmosphere.

Density measurements were performed at room temperature with a helium-based gas displaced pycnometer, type Micromeritics AccuPyc 1330. Samples of about 2 g were grinded to avoid entrapped bubbles in the polymer matrix and analyzed in 10 successive runs.

The fracture toughness of the cured nanocomposites was determined according to the compact tension method ASTM E-399 on an Instron 4486 universal tester. Specimens were pre-cracked prior to testing by inserting a razor blade into the machined notch and impacting with a hammer. After placing the specimen in a jig, the samples were tested at a crosshead speed of 1.3 mm/min.

The flexural properties of the series of nanocomposites were determined following the ASTM standard D790M-93. Samples of $80 \times 10 \times 4\ \text{mm}^3$ were supported over a span of 64 mm and bent with a crosshead motion of 1.0 mm/min. The force was recorded with a 1 kN load cell. The flexural modulus was calculated from the gradient in load vs. displacement curve according to the classical beam theory.

Electronically recorded optical micrographs were obtained from a Leica DMRM microscope. Atomic force microscopy (AFM) images were recorded using a Digital Instruments Nanoscope IIIa scanning probe microscope in the phase contrast mode.

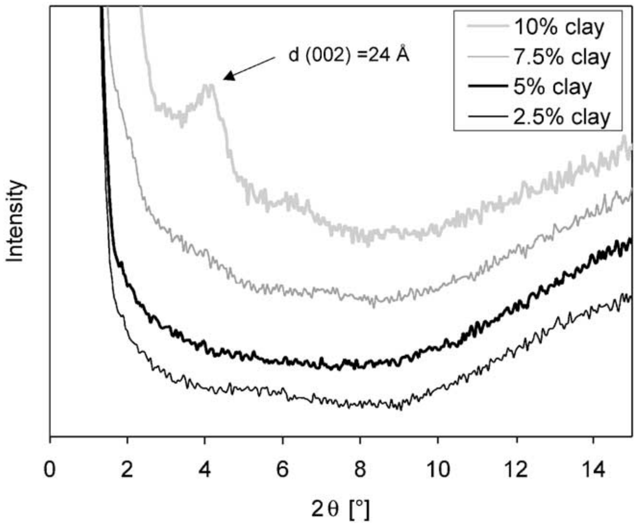

Fig. 1. WAXS of DETDA cured DGEBA nanocomposites containing 0–10% organoclay.

3. Results and discussion

3.1. Morphology

A wide range of epoxy nanocomposites containing 0, 2.5, 5, 7.5 and 10% organoclay were prepared. The morphology of the cured samples was investigated using wide-angle X-ray scattering (WAXS), as well as different microscopy techniques. WAXS traces of the clay concentration series show that the organoclay with an initial *d*-spacing of 23 Å is mainly exfoliated in the DGEBA-based system (Fig. 1). Only the DGEBA nanocomposite of the highest organoclay concentration (10%) shows a distinct peak correlating to a *d*-spacing of 48 Å. In contrast to the DGEBA-based systems, resins of higher functionality show distinctive peaks even at lower organoclay concentrations, indicating that these samples have a lower degree of exfoliated layered silicate. WAXS traces are shown in Fig. 2 for TGAP and

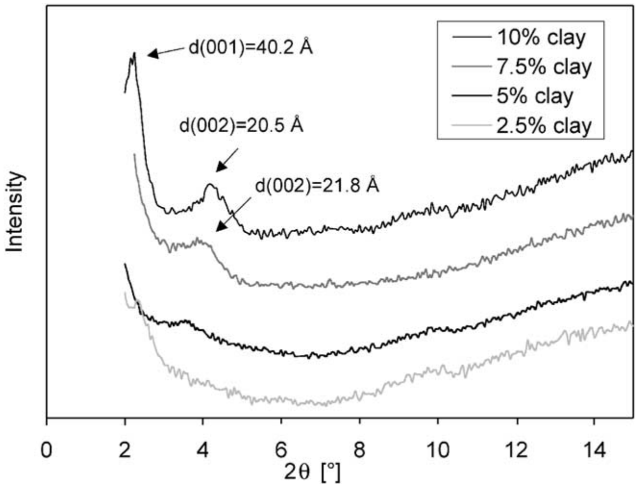

Fig. 2. WAXS of DETDA cured TGAP nanocomposites containing 0–10% organoclay.

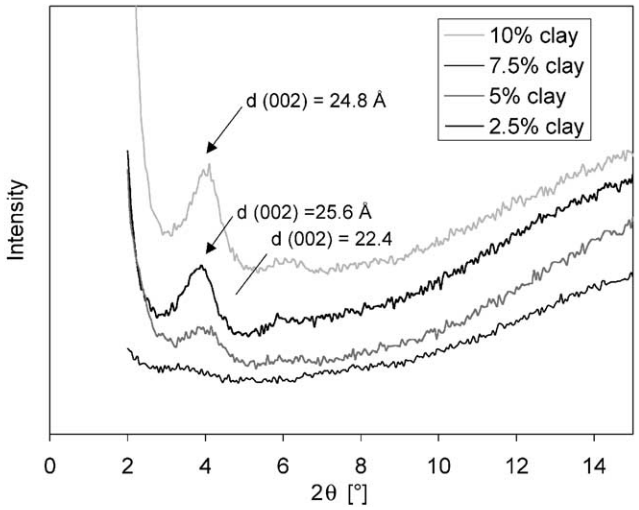

Fig. 3. WAXS of DETDA cured TGDDM nanocomposites containing 0–10% organoclay.

Fig. 3 for TGDDM. In any event, the peak observed around 25 Å or $2\theta = 4°$ correlates to the 002 plane and therefore represents only half the distance of the d-spacing.

Before investigating the microstructure of the nanocomposites, optical microscopy was applied to image the bulk surface. Optical micrographs as shown in Fig. 4 for the DGEBA system containing 5 wt% organoclay, show large particulate phases, indicating that even for the DGEBA-based system not all clay particles are fully dispersed in the polymer phase.

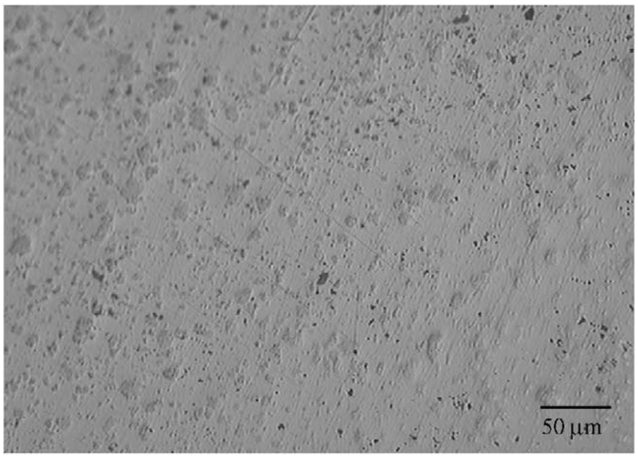

Fig. 4. Optical micrograph showing large particles the DETDA cured DGEBA system containing 5% organoclay.

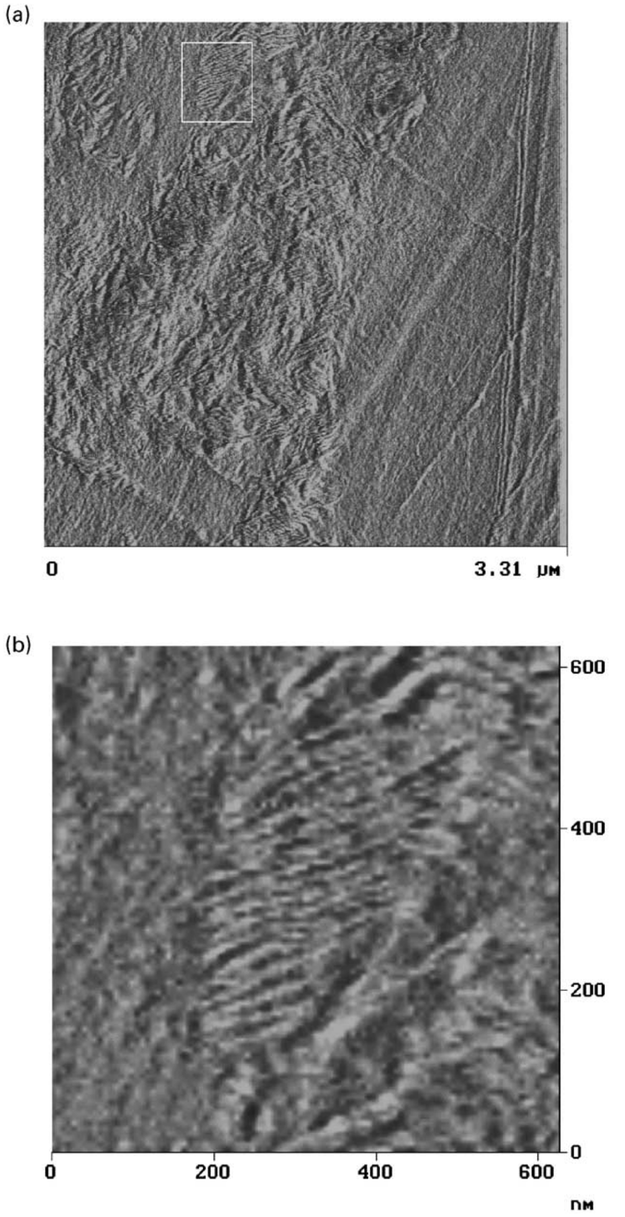

Fig. 5. Phase contrast AFM images of DETDA cured DGEBA containing 5% organoclay.

AFM was found to be a powerful tool to investigate the nanocomposite surface on a micrometer [22,23] and in some cases even on a nanometer scale [9,10]. Fig. 5(a) and (b) shows AFM phase contrast images of the DGEBA nanocomposite containing 5% layered silicate. Fig. 5(b) represents a higher magnification of the selected area shown in Fig. 5(a). Individual layers cannot be seen by AFM as they usually are by transmission electron microscopy (TEM). A striated structure, however, can be seen with increasing phase intervals at the top of the picture. Both, optical microscopy and AFM images show that at least part of the silicate content remains in tactoids or stackings of layers rather than forming a homogenous morphology through the whole material. Previous work by Zilg et al. [9] has pointed out that different tools such as TEM, AFM and WAXS may give a different picture of the state of morphology. They demonstrated that TEM has shown some large interlayer distance for a Jeffamine based nanocomposite whilst WAXS measurements indicated a smaller interlayer distance in the same system. Also in their work comparison between AFM and WAXS results for a particular nanocomposite did show a discrepancy of the interlayer distance of 40 Å. This indicates that different size

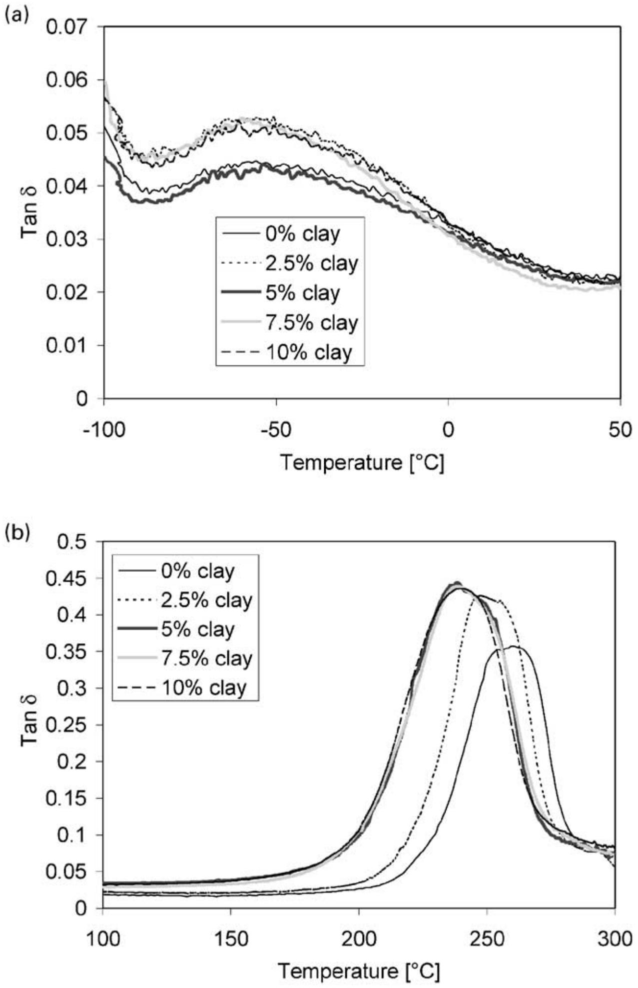

Fig. 6. Typical DMTA spectrum of TGDDM-based nanocomposites at 1 Hz; (a) subambient and (b) superambient temperatures.

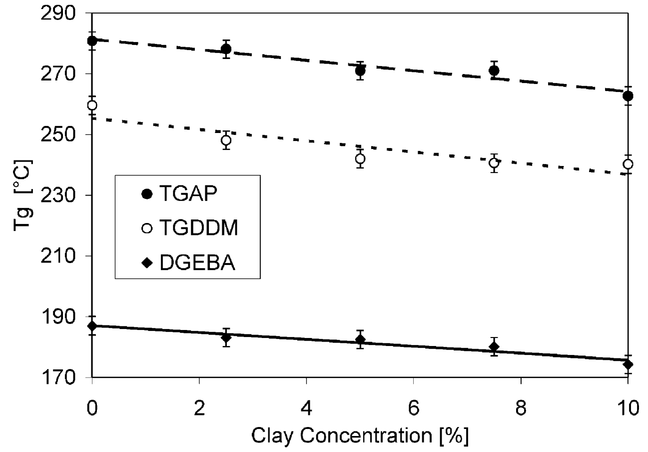

Fig. 7. Glass transition temperatures as determined from the tan δ peak of DMTA measurements.

scales and issues of self-similarity of structures formed becomes an issue. Since any of these methods investigates only a small volume of the bulk material, conclusions on the overall morphology can only be made carefully.

Dynamic mechanical thermal analysis was applied in two steps from -100 to 50 °C and from 50 to 300 °C to investigate the influence of the organoclay on the α- and β-transition. It is likely that these motions can be affected by the organoclay by being influenced by the surface of the silicate. Indeed, Beall [24] claims that in thermoplastic materials, for a concentration of 5% exfoliated clay, some 50% of the polymer chains are affected by the organoclay surface.

The α-transition is related to the Brownian motion of the main-chains at the transition from the glassy to the rubbery state and the relaxation of dipoles associated with it. The β-transition occurs at significantly lower temperatures and has been widely reported to be related to the crankshaft rotation of the hydroxy ether segments ($-CH_2-CH(OH)-CH_2-O-$) of the crosslinked network in the glassy state [25,26]. When a polymer goes through one of these relaxations, tan δ, the ratio of energy dissipated to energy stored, shows a maximum and provides a very sensitive means of analyzing the α- and β-relaxations. A typical DMTA tan δ trace is shown for the TGDDM/DETDA/organoclay system for different compositions at 1 Hz. Fig. 6(a) shows measurements for subambient temperatures and Fig. 6(b) represents those relaxations at superambient temperatures. Quite clear relaxation peaks can be observed in both cases.

Plots of the glass transition temperature (T_g) as a function of organoclay concentration are shown in Fig. 7. The value of T_g decreased steadily with increasing organoclay concentrations. The reduction in T_g was found to be in the order of 15 °C for the TGAP and DGEBA-based system and 20 °C for the TGDDM-based system at an organoclay content of 10%.

The glass transition temperatures of DGEBA-based epoxy nanocomposite systems have been investigated previously [6,9,12,15,19,27–31]. Whilst increased glass transition temperatures were reported in some cases of intercalated nanocomposite systems [6,15,27,28], others have found a constant or slightly decreased [29–30] T_g. Zilg et al. [9,19] have found that effectively intercalated epoxy systems significantly decrease the T_gs of the final resin system. Since it is a decrease it indicates that it is not an ‘adsorbed layer’ effect as this usually increases the glass transition temperature due to chains being tied down by the surface of the silicate. It has been found by Giannelis [32] that the T_g of intercalated polymers as characterized by solid-state NMR, show a reduced value of glass transition due to the lack of surrounding entanglements. However, since this system is rather more complex, with a range of chemistries possible, it is much more difficult to identify reasons. The clay may change the chemistry of the reaction, as has been shown earlier [33] and indeed the organo-ions themselves may catalyze homopolymerization, although this is unlikely to produce the high crosslink density of the epoxy–amine reaction. In addition unreacted resin plactization and a general lower crosslink density are reasons that there could be a decrease in T_g. It was assumed that the T_g

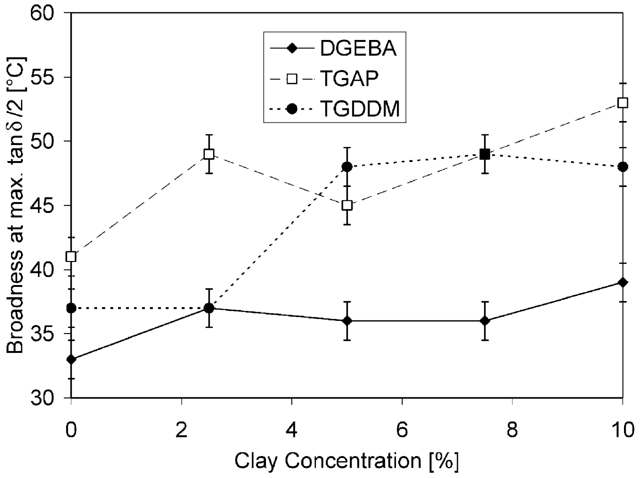

Fig. 8. Tan δ broadness at half peak height vs. nanocomposite composition.

was reduced due to a combination of factors. This complexity does not allow a precise determination of the governing factors, which decreases the glass transition temperature.

The broadness of the α-relaxation peak was determined at the half height of the peak and is shown in Fig. 8. The unfilled systems are generally less broad than the organoclay containing epoxy resins. Although results show some scattering, traces follow a general trend of increasing tan δ peak broadness with increasing clay concentration. The broadening of the α-relaxation might be related to restrained chain mobility that usually occurs in compatible blends, making the chain mobility more difficult and therefore covering a wider temperature range [34]. It can be assumed that molecules that are located close to or even tethered to the silicate show a different mobility than those molecules that are fully embedded in an epoxy environment, and that the concentration of epoxy molecules associated with the clay layers is actually quite high.

As shown in Fig. 9, the temperature location of the β-relaxation peak for each nanocomposite system also decreases steadily with increasing organoclay content. The decrease in the β-transition temperature is consistent although less significant than the reduction in the glass transition peak. The β-relaxation peaks are shifted by some 5–7 K through the addition of 10% organoclay. Since the peaks are generally very broad and weak with regards to intensity, (compare Fig. 6(a)) variations in the peak broadness are more difficult to determine. The TGDDM (Fig. 6(a)) and TGAP-based systems do not exhibit significant changes in the β-relaxation broadening over the different organoclay concentrations. The DGEBA-based nanocomposites, however, shows notable broadening at organoclay concentrations of 7.5 and 10%. Previous work by the group of Monnerie and Halary [26,35–38] has focused on the secondary relaxation of epoxy resin systems. It was reported that an increase in crosslink density (as varied by different hardeners of different functionalities) increases the peak height and broadening of the secondary relaxation whilst changes in chain flexibility showed little effect on the viscoelastic response [35]. Imaz et al. [39] have studied the β-transition of a TGDDM-based system as a function of crosslink density. In contrast to the work of Monnerie and Halary an increase in the peak temperature was found with increasing crosslink density. In summary for our systems it appears that incorporation of clay leads to a decrease in both the glass transition and secondary relaxation temperatures, possibly due to a decrease in effective crosslink density. The fact that it influences the β-relaxation which involves mobility in the glassy state indicates that the change is significant and that—as previous works quoted earlier have shown—the β-relaxation does involve a degree of cooperative motion rather than very localized mobility only.

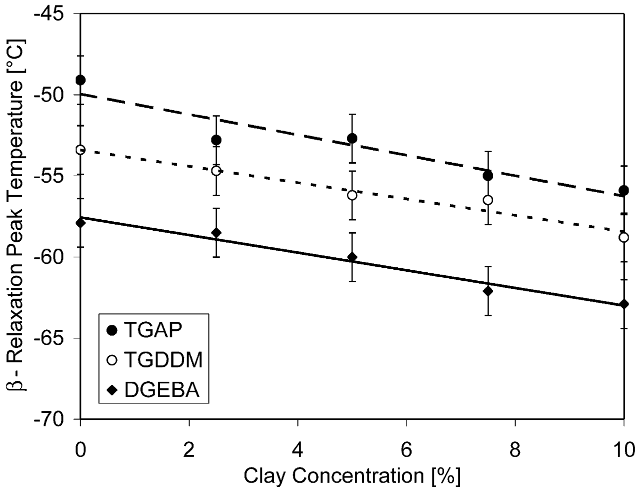

Fig. 9. β-Relaxation peak temperatures as determined from subambient DMTA measurements.

Further investigations of the cured nanocomposite series were undertaken to assess the degree of cure of the materials being investigated. DSC thermograms were taken for all postcured samples to determine if any further reaction could be detected, despite postcuring. Peak temperatures and %residual cure of these DSC scans are summarized in Table 2. Whilst the DSC traces for the DGEBA-based systems confirmed full cure, the TGAP and TGDDM-based nanocomposites show small peaks around 250 °C indicating further reaction. Although the amount of reaction is very little, the filled resin was more fully cured than neat systems. Thus it does not appear that the nanocomposites show lower cure, indeed the degree of thermal cure seems high. It still does not mean that the architecture of the resulting network is not such that there are lower crosslink density regions, perturbed by the presence of the clay. Within these regions there may still be unreacted groups, cyclized units or etherified groups that do not contribute as much to crosslink density as epoxy–amine reactions.

One of the key benefits of epoxy materials is their low density. Hence it was of interest to us how the materials density changed with filler addition. Density results of the

Table 2
DSC results of postcured epoxy–nanocomposite systems

Clay conc. (%)	TGAP		TGDDM	
	Peak (°C)	%Residual cure	Peak (°C)	%Residual cure
0	266.4	5.1	253.7	4.3
2.5	270.2	2.9	237.4	0.7
5	251.0	3.0	248.5	3.7
7.5	253.7	2.8	233.0	1.1
10	255.7	1.6	229.5	0.6

various nanocomposites after postcure as determined by gas-displacement pycnometry are shown in Fig. 10. Theoretical densities according to the rule-of-mixture were calculated based on an organoclay density of 1.6748 g/cm^3 (as determined by the same method). The rule-of-mixture data are represented as straight lines in Fig. 10. It can be noticed that all densities are within a very small range of 1.1925–1.2307 g/cm^3. Therefore the variation in specific weight due to the filler content is not a drawback for technical applications. It is interesting to see that densities are generally slightly below predicted values following the rule-of-mixture. The lower density is possibly related to poorer packing of the polymer molecules near the silicate layers. However, free volume and molecular packing of these materials is not the main focus of this paper and will be discussed in more detailed elsewhere [40].

3.2. Mechanical properties

For each set of nanocomposites the modulus was determined using the three-point bend test. Modulus results are shown in Fig. 11. All resin systems show a monotonic increase in modulus with increasing organoclay concentrations. The normalized modulus was calculated by dividing the actual nanocomposite modulus value through the modulus of the unfilled system. In Fig. 12 it can be seen that the increase in modulus for all resin systems is in a range of 20% for an organoclay concentration of 10%. The improved stiffness can be directly ascribed to the reinforcement of the exfoliated high aspect ratio platelets [41]. It is assumed [8,9] that the reinforcement provided through exfoliation is due to shear deformation and stress transfer in the platelet particles.

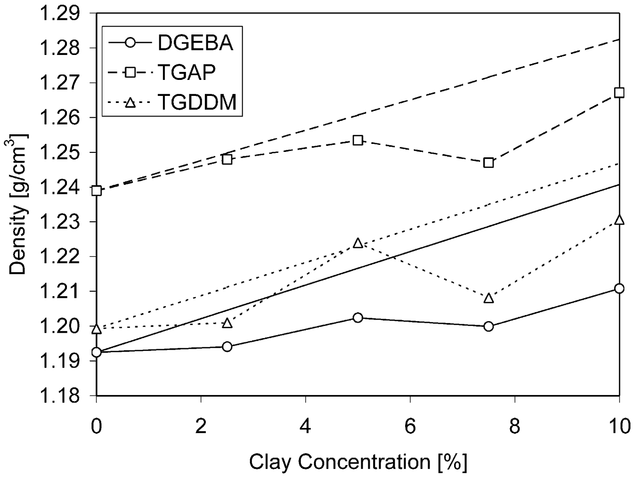

Fig. 10. Density of cured epoxy nanocomposites as determined from gas displaced pycnometry. The dotted lines represent theoretical densities according to the rule-of-mixture.

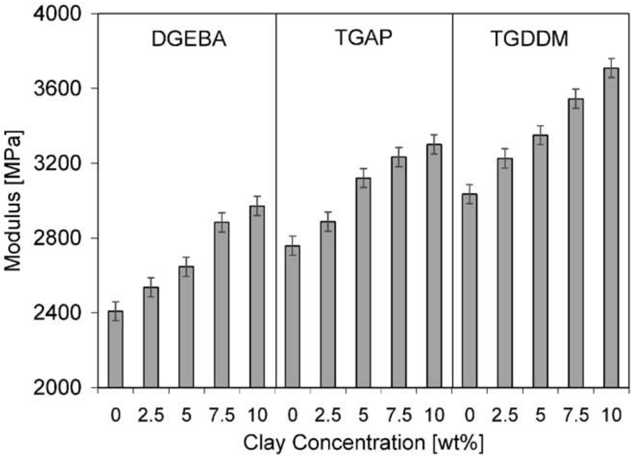

Fig. 11. Modulus of different DETDA cured resins containing 0–10% organoclay.

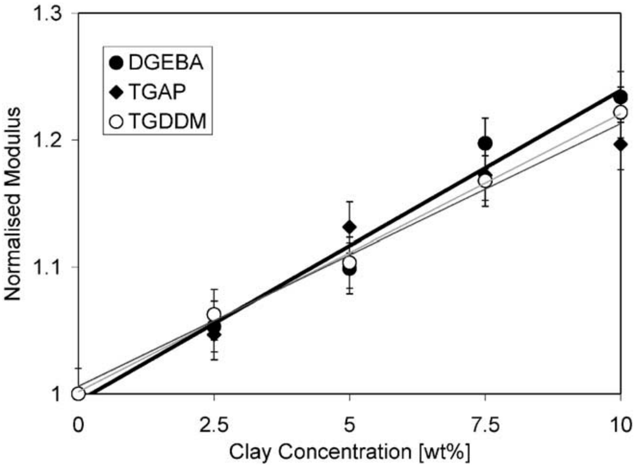

Fig. 12. Normalized modulus of different DETDA cured resins containing 0–10% organoclay.

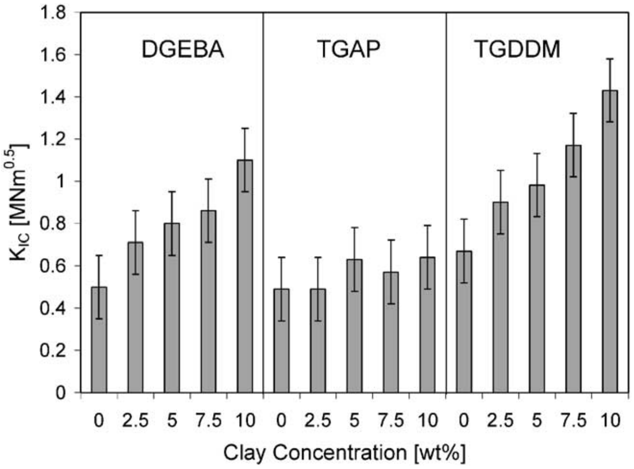

Fig. 13. Stress intensity factor of different DETDA cured resins containing 0–10% organoclay.

Highly flexible and low glass transition resins are often thought to achieve better improvements in materials performance in comparison to rigid, highly crosslinked resins. In the prior work by Lan and Pinnavaia [8], it was found that a Jeffamine D2000 cured DGEBA nanocomposite increased the modulus by approximately 500% at an organoclay concentration of 10 wt%. The DGEBA system in our work shows only slightly greater relative improvements in modulus than the TGAP or TGDDM resin, respectively. However, all of these resin systems have a high glass transition temperature and are deep in the glassy state at room temperature.

The fracture toughness, as quantified by the stress intensity factor, K_{IC}, was determined using the compact tension test. Results for the K_{IC} values are shown in Figs. 13 and 14, respectively, for the normalized stress intensity factor. Whilst most toughening techniques show a loss in stiffness (such as rubber toughened epoxy resins [42]), it can be seen that both, toughness and stiffness have been improved through the organoclay incorporation. The stress intensity factor indicates that DGEBA and TGDDM show an increase in toughness in a similar range, whilst improvement in the TGAP systems is significantly lower. Research by Zilg et al. [9] proposed that intercalated clay promotes toughness whereas exfoliated clay platelets mainly improve stiffness of the polymer matrix, due to energy-absorbing shearing of intercalated clay layers. It must be recalled that these materials do have a lateral dimension in the micron scale and it is possible that these may encourage crack stopping and pinning.

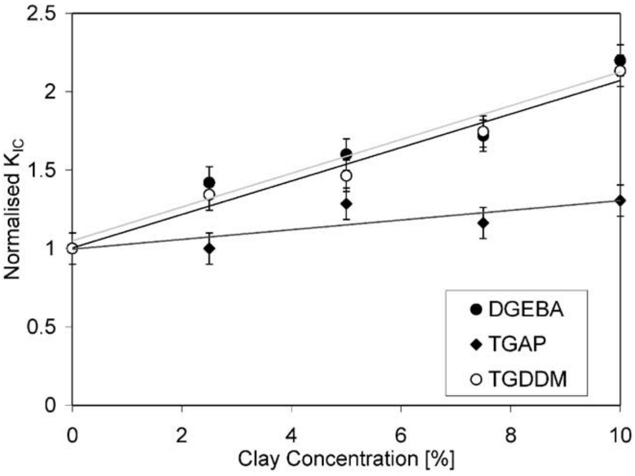

Fig. 14. Normalized stress intensity factor of different DETDA cured resins containing 0–10% organoclay.

Our morphology studies have shown that the arrangement of the silicate layers cannot neatly be termed as either intercalated or exfoliated. It is likely that the overall structure of the nanocomposites is a blend of intercalated and exfoliated organoclay layers.

4. Conclusion

Comparison of WAXS and AFM analysis of the organoclay morphology in the various polymer matrices in this work has shown that there is not a simple, idealized nanocomposite morphology, but rather a combination of intercalated and exfoliated structures. Care thus has to be taken when deducing morphology from micrographs or WAXS results. In the literature many reports of work can be found where an attempt is made to reach full exfoliation of the organoclay. Such exfoliation during in situ polymerization may not make it possible to form a true, fully homogeneous exfoliated nanocomposite.

Investigation of the temperature location of the α- and β-transition have shown a steady decrease of both with increasing organoclay content. Broadness is affected in the case of the primary relaxation, but not the secondary one. The reduced temperature indicates a possible lower crosslink density around the clay particle, perhaps due to the perturbing effects of the clay, even though the presence of the clay encourages higher conversion of the epoxy. Since the T_g measured is a bulk process it appears that the fine dispersion of the nanometer-thick clay platelets influences much of the volume of epoxy matrix.

Improvement in stiffness of the high-functionality epoxy resins is comparable with those achieved for the bifunctional (DGEBA) resin system [9]. Although it is often found that improvement in modulus sacrifices toughness of the material, both toughness and stiffness could be improved through the incorporation of organoclay. This has been reported previously for the bifunctional DGEBA nanocomposite systems and also applies for epoxy systems of higher functionalities, TGAP and TGDDM. The improved modulus and toughness makes the nanocomposite strategy an attractive alternative to the commonly used micron-sized fillers.

Acknowledgments

The Dr Jürgen-Ulderup Foundation, the German National Merit Foundation and the Australian Research Council are gratefully acknowledged for financial support. Mr Lee Brunckhorst and Dr Geoff Spinks of the University of Woolongong are acknowledged for production of optical micrographs and atomic force microscopy images.

References

[1] Solomon DH, Hawthorne DG. Chemistry of pigments and fillers. New York: Wiley; 1983.

[2] Hawley GC. In: Milewski JV, Katz HS, editors. Handbook of reinforcements for plastics. New York: Van Nostrand Reinhold Company; 1987.

[3] Usuki A, Kojima Y, Kawasumi M, Okada A, Fukushima Y, Kurauchi T, Kamigaito O. J Mater Res 1993;8:1179–84.

[4] Usuki A, Kojima Y, Kawasumi M, Okada A, Fukushima Y, Kurauchi T, Kamigaito O. J Mater Res 1993;8:1185–9.

[5] Kornmann X, Lindberg H, Berglund LA. Polymer 2001;42(4): 1303–10.

[6] Brown JM, Curliss D, Vaia RA. Chem Mater 2000;12:3376–84.

[7] Wang MS, Pinnavaia TJ. Chem Mater 1994;6(4):468–74.

[8] Lan T, Pinnavaia TJ. Chem Mater 1994;6(12):2216–9.

[9] Zilg C, Mülhaupt R, Finter J. Macromol Chem Phys 1999;200(3): 661–70.

[10] Chin I-J, Thurn-Albrecht T, Kim C-H, Russell TP, Wang J. Polymer 2001;42:5947–52.

[11] Wang Z, Pinnavaia JT. Chem Mater 1998;10(7):1820–6.

[12] Lee A, Lichtenhan JD. J Appl Polym Sci 1999;73(10):1993–2001.

[13] Wang Z, Lan T, Pinnavaia JT. Chem Mater 1996;8(9):2200–4.

[14] Lan T, Kaviratna PD, Pinnavaia TJ. Chem Mater 1995;7(11): 2144–50.

[15] Messersmith PD, Giannelis EP. Chem Mater 1994;6(10):1719–25.

[16] Lan T, Kaviratna PD, Pinnavaia TJ. Polym Mater Sci Engng 1994;71: 527–8.

[17] Ke Y, Lü J, Yi X, Zhao J, Qi Z. J Appl Polym Sci 2000;78(4):808–15.

[18] Jiankun L, Yucai K, Zongneng Q, Xiao-Su Y. J Polym Sci, Part B: Polym Phys 2001;39:115–20.

[19] Zilg C, Thomann R, Finter J, Mülhaupt R. Macromol Mater Engng 2000;280/281:41–6.

[20] Kornmann X, Lindberg H, Berglund LA. Polymer 2001;42(10): 4493–9.

[21] Guerrero P, De la Caba K, Valea A, Corcuera MA, Mondragon I. Polymer 1996;37(11):2195–200.

[22] Feng J, Weng L, Chan C, Xhie J, Li L. Polymer 2001;42:2259–62.

[23] Reichert P, Nitz H, Klinke S, Brandsch R, Thomann R, Mülhaupt R. Macromol Mater Engng 2000;275:8–17.

[24] Beall GW. New conceptual model for interpreting nanocomposite behavior. In: Pinnavaia TJ, Beall GW, editors. Polymer–clay nanocomposites. Chichester: Wiley; 2000. p. 267–79.

[25] Pogany GA. Polymer 1970;11:66–78.

[26] Lautrêtre F, Eustache R-P, Monnerie L. Polymer 1995;36(2):267–74.

[27] Lee DC, Jang LW. J Appl Polym Sci 1997;68:1997–2005.

[28] Kelly P, Akelah A, Qutubuddin S, Moet A. J Mater Sci 1994;29: 2274–80.

[29] Massam J, Pinnavaia TJ. Clay nanolayer reinforcement of a glassy epoxy polymer. Mater Res Soc Symp Proc 1998;.

[30] Bajaj P, Jha NK, Ananda Kumar R. J Appl Polym Sci 1990;40: 203–12.

[31] Tak Gam K., Sue H.J. Preparation and Mechanical Properties of Epoxy-Clay nanocomposites in ACS Spring Meeting. 2000 San Francisco.

[32] Zax D, Yang D, Santos R, Hegemann H, Giannelis H, Manias E. J Chem Phys 2000;112(6):1951–2945.

[33] Becker O, Simon G, Varley R, Halley P. Submitted for publication.

[34] Lin M-S, Lee S-T. Polymer 1997;38(1):53–8.

[35] Cukierman S, Halary J-L, Monnerie L. Polym Engng Sci 1991;31(20): 1476–82.

[36] Heux L, Laupretre F, Halary JL, Monnerie L. Polymer 1997;39(6–7): 1269–78.

[37] Heux L, Halary JL, Laupretre F, Monnerie L. Polymer 1997;38(8): 1767–78.

[38] Bershtein VA, Peschanskaya NN, Halary JL, Monnerie L. Polymer 1999;40:6687–98.

[39] Imaz J-J, Juvado M.J, Corcuera M.A, Mondragon I. J Appl Polym Sci 1992;46:147–66.

[40] Becker O, Simon GP, Varley R. Unpublished data.

[41] Wang Z, Massam J, Pinnavaia TJ. Epoxy–clay nanocomposites. In: Pinnavaia TJ, Beall GW, editors. Polymer–clay nanocomposites. Chichester: Wiley; 2000. p. 127–48.

[42] Sankaran S. J Appl Polym Sci 1990;39:1635–47.